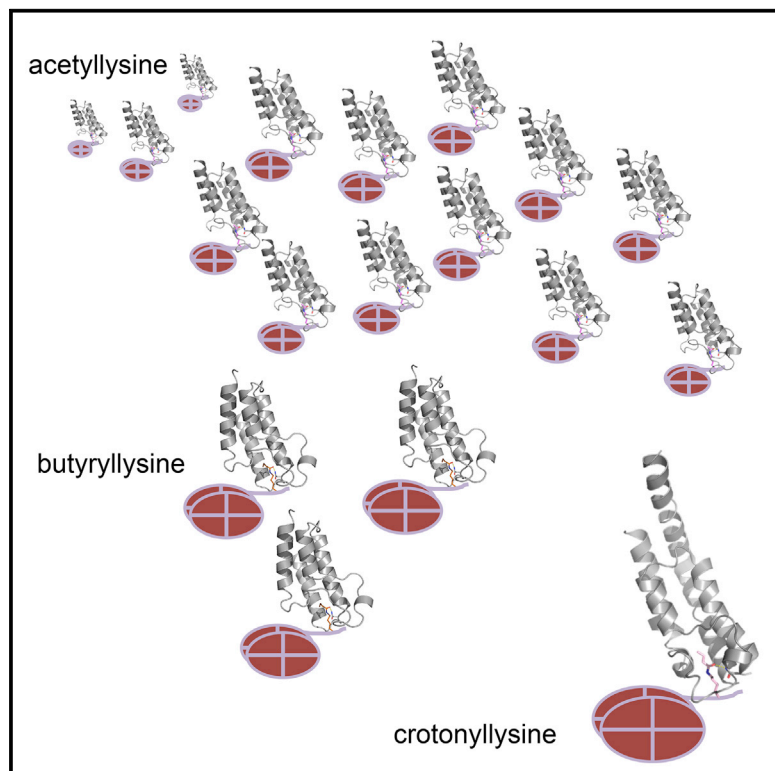# Structure

A Subset of Human Bromodomains Recognizes Butyryllysine and Crotonyllysine Histone Peptide Modifications

Graphical Abstract

Authors

E. Megan Flynn, Oscar W. Huang, Florence Poy, ..., Steve F. Bellon, Yong Tang, Andrea G. Cochran

Correspondence

cochran.andrea@gene.com (A.G.C.), yongtang@broadinstitute.org (Y.T.)

In Brief

Bromodomains are protein modules that "read" acetyllysine marks on histone tails. Flynn et al. screen human bromodomains for binding to less common histone acyl modifications and find candidate bromodomain readers for butyryl- and crotonyllysine. Crystal structures reveal how these unusual modifications are accommodated.

Highlights

- BRD9 and CECR2 bromodomains bind to butyryllysine

- The second bromodomain of TAF1 binds to butyryl- and crotonyllysine

- Crotonyllysine binding rearranges conserved water molecules

Accession Numbers

4YY4
4YYI
4YYJ
4YYK
4YY6
4YYG
4YYD
4YYH
4YYM
4YYN

CrossMark

CellPress

A Subset of Human Bromodomains Recognizes Butyryllysine and Crotonyllysine Histone Peptide Modifications

E. Megan Flynn,[1] Oscar W. Huang,[1] Florence Poy,[2] Mariano Oppikofer,[1] Steve F. Bellon,[2] Yong Tang,[2,3,*] and Andrea G. Cochran[1,*]

[1]Department of Early Discovery Biochemistry, Genentech, Inc., 1 DNA Way, South San Francisco, CA 94080, USA
[2]Department of Structural Biology, Constellation Pharmaceuticals, Inc., 215 First Street, Suite 200, Cambridge, MA 02142, USA
[3]Present address: Center for the Development of Therapeutics, Broad Institute of MIT and Harvard, 415 Main Street, Cambridge, MA 02142, USA
*Correspondence: cochran.andrea@gene.com (A.G.C.), yongtang@broadinstitute.org (Y.T.)
http://dx.doi.org/10.1016/j.str.2015.08.004

SUMMARY

Bromodomains are epigenetic readers that are recruited to acetyllysine residues in histone tails. Recent studies have identified non-acetyl acyllysine modifications, raising the possibility that these might be read by bromodomains. Profiling the nearly complete human bromodomain family revealed that while most human bromodomains bind only the shorter acetyl and propionyl marks, the bromodomains of BRD9, CECR2, and the second bromodomain of TAF1 also recognize the longer butyryl mark. In addition, the TAF1 second bromodomain is capable of binding crotonyl marks. None of the human bromodomains tested binds succinyl marks. We characterized structurally and biochemically the binding to different acyl groups, identifying bromodomain residues and structural attributes that contribute to specificity. These studies demonstrate a surprising degree of plasticity in some human bromodomains but no single factor controlling specificity across the family. The identification of candidate butyryl- and crotonyllysine readers supports the idea that these marks could have specific physiological functions.

INTRODUCTION

Among the many post-translational modifications on histone tails, lysine acetylation is highly abundant and produces profound biological effects (Choudhary et al., 2009; Kouzarides, 2000; Norris et al., 2009). Neutralization of the charge of the N^6-amino group is believed to disrupt the interaction between histones and DNA, which in turn changes nucleosome dynamics and DNA accessibility and, ultimately, gene expression (Kouzarides, 2007). Lysine acetylation also recruits chromatin remodeling proteins and transcription factors through a small acetyllysine-binding module called the bromodomain (Haynes et al., 1992; Dhalluin et al., 1999; Owen et al., 2000). Abnormal protein acetylation may deregulate transcription in cancer and other diseases, prompting efforts to discover small-molecule inhibitors targeting enzymes that add or remove the acetyl group, namely the histone acetyltransferases (HATs) and histone deacetylases (HDACs), respectively (Furdas et al., 2012; Lane and Chabner, 2009; Shahbazian and Grunstein, 2007). Likewise, bromodomain-containing proteins have been implicated in disease, prompting interest in bromodomain modulation by small molecules (Chung, 2012; Filippakopoulos and Knapp, 2014; Hewings et al., 2012; Sanchez et al., 2014).

The activated acetyl group transferred to lysine by HATs is carried by acetyl coenzyme A (acetyl-CoA). Acetyl-CoA is required for biosynthesis of many biomolecules and is a feedstock for the citric acid cycle. Acetyl-CoA is also a central intermediate in metabolism and is produced by pathways that process fatty acids, sugars, and amino acids. The latter pathways proceed, in part, through conversion of a series of short-chain acyl-CoA intermediates, eventually leading to acetyl-CoA or important intermediates, such as succinyl-CoA. Each of these activated CoA intermediates is, in principle, an acyl donor to lysine.

Intriguingly, it has been found through sensitive mass spectrometry methods that a number of non-acetyl acyl modifications are present on histone lysine residues (Arnaudo and Garcia, 2013; Olsen, 2014). The current catalog of these alternative lysine acylations includes formylation (Jiang et al., 2007; Wisniewski et al., 2008), propionylation (Chen et al., 2007; Liu et al., 2009; Tweedie-Cullen et al., 2012; Zhang et al., 2009), butyrylation (Chen et al., 2007; Tweedie-Cullen et al., 2012; Zhang et al., 2009), crotonylation (Tan et al., 2011; Tweedie-Cullen et al., 2012), 2-hydroxyisobutyrylation (Dai et al., 2014), succinylation (Weinert et al., 2013; Xie et al., 2012), malonylation (Xie et al., 2012), and glutarylation (Tan et al., 2014) (Figure 1A). It is not presently understood whether these modifications have specific physiological functions. One possibility is that they may instead represent a form of metabolic noise: this could result either from non-selective introduction by HATs or from chemical reactivity of acyl-CoA (Wagner and Payne, 2013; Weinert et al., 2013). On the other hand, it has been reported recently that the HAT p300 can introduce crotonyl histone modifications and that these support transcriptional activation in a manner similar to acetyl modifications (Sabari et al., 2015).
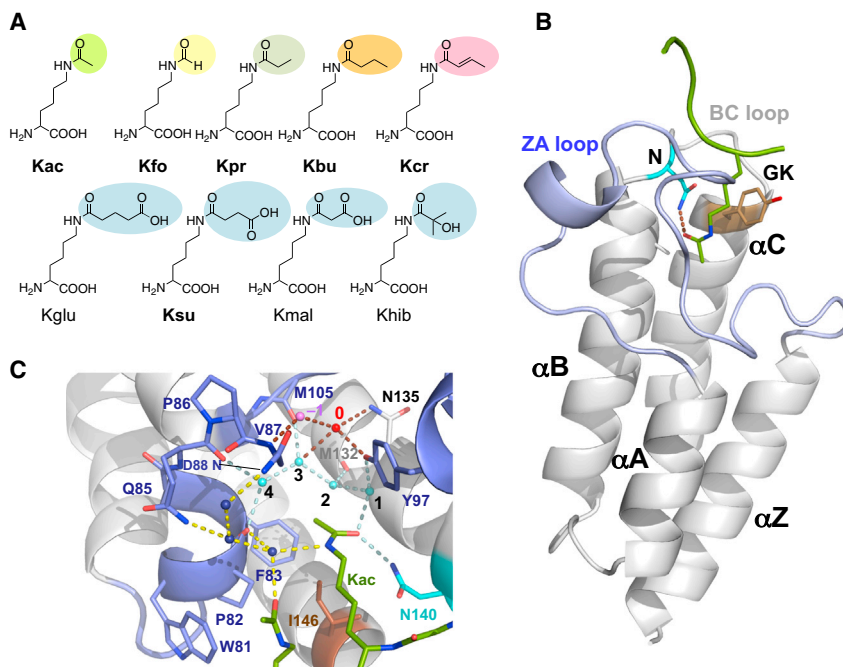
Figure 1. Acyl Marks and Bromodomains

(A) Chemical structures of histone acyllysine modifications. The colored ovals highlight the acyl group. Lysine modifications and abbreviations are: acetyl (Kac), formyl (Kfo), propionyl (Kpr), butyryl (Kbu), crotonyl (Kcr), glutaryl (Kglu), succinyl (Ksu), malonyl (Kmal), and hydroxyisobutyryl (Khib). Those indicated in bold type were evaluated in the studies reported here, and those shown in colors other than blue bound to at least one human bromodomain. The color scheme for Kac, Kpr, Kbu, and Kcr is maintained in figures throughout. See also Figure S1.

(B) Cartoon representation of a bromodomain (here, that of BRD9) showing secondary structural elements and other features. The long ZA loop is shown in blue. The critical asparagine "anchor" residue (N; cyan) hydrogen bonds to bound acetyllysine (peptide shown in green). An important specificity-determining residue is the "gatekeeper" (GK) (brown; see text and partial sequence alignment of Figure 5A).

(C) Detailed view of the BRD4(1) binding site (PDB: 3UVW; Filippakopoulos et al., 2012) focusing on conserved water networks. The color scheme is taken from (B), but the orientation is different; a portion of the ZA loop (residues 88–95) has been omitted to aid in viewing the ligand pocket. In addition to the gatekeeper (I146) and the anchor (N140), the nearly invariant Y97 and N135 and "WPF shelf" residues W81, P82, and F83 are shown. Several structurally well-defined water molecules are depicted as small numbered spheres. We adopt the water numbering of a recent review (Hewings et al., 2012) for waters 1–4 and include "water 0" (shown in red) and "water −1" (shown in pink) among structurally important and conserved waters. Water 0 is not immediately adjacent to Kac ligand, nor is it generally discussed in published papers. Nevertheless, it appears to be among five conserved (but not explicitly defined) binding-site waters considered important in a recent computational study (Vidler et al., 2012). Water 0 is the center of a dense network of interactions (pink dotted lines) and bridges residues Y97 and N135, linking them either to water 2 (as in BRD9 structures, see Figure 3A) or water 3 (here). Water −1 bridges water 0 and the amide of V87. Water −1 is not ubiquitous in bromodomain structures but it is very commonly seen and, although not depicted in some of the subsequent figures, it is present in the structures reported here. The light-blue spheres (with interactions shown in light blue) correspond to the four canonical waters (1–4) most commonly discussed; water 1 bridges the Kac carbonyl oxygen to Y97. Dark-blue spheres (interactions indicated in yellow) correspond to additional "ZA channel" waters (Hewings et al., 2012), and are shown here to differentiate from the location and network of water 0. The center of the three ZA channel waters shown (that interacting with the side chain of Q85) has been proposed as "the fifth conserved water molecule" and numbered as either water 5 or water 6 in accompanying figures (Hewings et al., 2012).

The case for function, even if deleterious, of non-acetyl acyl marks is strengthened by reports that a subset of the sirtuin-family HDACs preferentially removes either acidic acyl modifications (malonyl [Du et al., 2011], succinyl [Du et al., 2011; Park et al., 2013], glutaryl [Tan et al., 2014]; SIRT5) or long-chain fatty acyl modifications (SIRT6 [Feldman et al., 2013; Jiang et al., 2013]). In addition, short-chain fatty acyl modifications (propionyl, butyryl, crotonyl) can be removed by various sirtuins (Bao et al., 2014; Feldman et al., 2013; Garrity et al., 2007; Smith and Denu, 2007). Thus, these may be regulated (or regulatory) processes, further suggesting that these acyl marks should be "read" in some way by chromatin-associated proteins. A strong candidate for such an acyllysine reader is the bromodomain, but an initial evaluation of the BET-class bromodomains of BRD2 and BRD4 suggested that the potential for reading acyl groups larger than acetyl might be very limited (Vollmuth and Geyer, 2010).

Here, we report a broad survey of the capacity of human bromodomains to recognize non-acetyl acyllysine modifications. We find that only three bromodomains (and presumably two additional bromodomains of high sequence identity) bind to butyryllysine (Kbu) with high affinity. Intriguingly, two of these Kbu-binding bromodomains, those of BRD9 and CECR2, discriminate butyryllysine from crotonyllysine, and we explore the underlying mechanism through structures of BRD9 in complex with different acyllysine analogs. We find only the second bromodomain of TAF1 to be capable of high-affinity recognition of crotonyllysine (Kcr) and Kbu. The structure of the TAF1-Kcr complex reveals that the crotonyl group displaces two conserved, ordered water molecules present in the binding pocket, resulting in a rearranged water network. Finally, we identify residues required for butyryllysine recognition by the BRD9 and CECR2 bromodomains, and engineer this capacity into the BRD1 bromodomain.

RESULTS

Screening Human Bromodomains for Recognition of Acetyllysine and Other Acyllysine Marks

Peptide arrays have proved to be a powerful approach to identify specificities of epigenetic reader modules. A broad survey of human bromodomains on arrays revealed limited site specificity for acetyllysine recognition in histone peptides, some sensitivity to adjacent non-acetyl marks, and enhanced binding of BET-class bromodomains to multiply acetylated peptides (Filippakopoulos et al., 2012). To build on this work, we synthesized arrays focusing on acylation of N-terminal tail regions of histones H3 and H4 (residues 1–40 and 1–24, respectively). These arrays

included peptides of different length and, for each length, all single acetyllysine modifications and various combinations of multiple acetylations. Because binding to peptide arrays is a qualitative screen, we included site redundancy and context variation in the design to give greater confidence in recognition of a given acetyl mark, and to allow for different sequence specificities that might exist; this process resulted in a base set of 96 peptides (Table S1). Finally, we synthesized this base set of peptides with non-acetyl acyl modifications (Figure 1A) to probe the capacity of bromodomains to recognize them and for direct comparison to recognition of acetyllysine in the same peptide sequence. We screened a panel of 49 soluble human bromodomains (of the 61 in human; Table S2), representing all structural subfamilies.

As was observed earlier (Filippakopoulos et al., 2012), the majority of human bromodomains (including 35 of 49 screened here) bind peptides in an acetylation-dependent manner (Table S2). All bromodomains that we found capable of acetyllysine recognition also bind to propionyllysine peptides on the array (see Figure S1 for examples). This suggests that the earlier finding of BRD2 and BRD4 bromodomain recognition of propionyllysine (Vollmuth and Geyer, 2010) reflects a general capability of the family to bind modifications one carbon longer than acetyl.

The major exception to acetyl- and propionyllysine recognition is among the group of "non-canonical" bromodomains (10 of 49 screened here): these lack the highly conserved asparagine "anchor" residue that forms the major hydrogen bonding interaction with the acetyl carbonyl group (Figure 1B). Many non-canonical bromodomains have a tyrosine residue in the equivalent position, and in examples with reported crystal structures this substitution largely blocks the binding site (ASH1L, PBRM1(1), and SP100; Filippakopoulos et al., 2012) or favors a different binding site and histone mark (ZMYND11; Wen et al., 2014). Not surprisingly, this group of bromodomains was incapable of acetylation-dependent peptide binding. However, we found that the non-canonical second bromodomain of PHIP (abbreviated PHIP(2) and in an analogous manner hereafter for other multi-bromodomain proteins), bearing a threonine anchor, does bind to acetylated peptides and discriminates between lysine and acetyllysine peptides (Figure S1). This is consistent with the reported structure of this bromodomain bound to N-methylpyrrolidinone, an acetyllysine mimetic, and largely consistent with the accompanying peptide array profiling (Filippakopoulos et al., 2012). Intriguingly, it appears that PHIP(2) is capable of binding to formyllysine peptides (Figure S1 and Table S2), an observation unique to this bromodomain.

A Subset of Aromatic Gatekeeper Bromodomains Recognizes Butyryllysine

BRD2 and BRD4 bromodomains have very low affinity for butyryllysine (Kbu) peptides (Vollmuth and Geyer, 2010). However, we suspected that this might not be the case for all bromodomains. The asparagine anchor residue and structural water molecules present in the bottom of the BRD4(1) binding pocket (Figure 1C) are common features across the canonical bromodomain family. (The water molecules are of particular interest—see below; however, there are inconsistencies and/or lack of adequate definitions for the waters when comparing different publications. We therefore propose an extension of the most complete annotation

[Hewings et al., 2012] in Figure 1C.) Additional features of the binding site include the long and variable loop connecting the first (α_Z) and second (α_A) helices (ZA loop) and the short loop connecting the third (α_B) and fourth (α_C) helices (BC loop) (Figure 1B). Flanking the BC loop is the anchor residue (end of α_B) and a residue commonly known as the gatekeeper (Chung et al., 2011) at the beginning of α_C (Figure 1B). The gatekeeper is generally hydrophobic (Filippakopoulos et al., 2012) and interacts with both the aliphatic portion of the acetyllysine side chain and the acetyl group itself, forming one wall of the binding pocket. In most canonical bromodomains, including those from BRD2 and BRD4, the gatekeeper is β-branched (isoleucine or valine), and this branching appears to restrict the size of the deepest portion of the pocket, near where the acetyl group binds (Figure 1C). We were particularly interested in the remaining canonical bromodomains, those with leucine, phenylalanine, or tyrosine gatekeepers (Table S2; see also Figure 5A), as it seemed that their slightly larger binding pockets might accommodate a broader range of acyl modifications.

Array screening revealed that a subset of the bromodomains having tyrosine gatekeepers, those of CECR2 and BRD9 (Figure 2A) (and also TAF1(2); see below) appeared to bind strongly to butyrylated peptides. In contrast, CECR2 and BRD9 bromodomains appeared incapable of binding to crotonylated peptides (Figure 2A). Like the butyryl group, the crotonyl modification consists of a linear arrangement of four carbons and differs only in the presence of a double bond (Figure 1A). It is remarkable that CECR2 and BRD9 can apparently discriminate between these two highly similar acyl modifications; antibodies capable of discriminating these marks are not currently available (Gattner et al., 2013).

To validate binding to Kbu-containing peptides, we measured affinities for a representative peptide series (histone H4, residues 1–11 with different K5/K8 diacyl modifications; see Experimental Procedures) by isothermal titration calorimetry (ITC) (Figure 2B). These data indicate that BRD9 and CECR2 each bind the doubly modified Kac, Kpr, or Kbu peptide with similar affinities and stoichiometry (two bromodomains per peptide; one bromodomain per acyllysine), while, as reported previously (Vollmuth and Geyer, 2010), BRD4(2) binds only to Kac and Kpr peptides. In accord with results from the array screening, we detected no significant binding to the analogous Kcr peptide by ITC at the protein and ligand concentrations accessible. Taken together, the data indicate that both CECR2 and BRD9 recognize the Kbu modification and that they select against Kcr.

Structures of BRD9 Peptide Complexes Reveal a Flexible Ligand Pocket that Allows High-Affinity Binding of Butyryllysine

To gain insight into recognition of Kbu and discrimination against Kcr ligands by the BRD9 bromodomain, we solved co-crystal structures with diacyl-modified peptides, as well as a complex with DMSO (Table 1). BRD9 structures in complex are highly similar to the published structure of the unliganded domain (Filippakopoulos et al., 2012). In contrast to some BRD4(1) (Filippakopoulos et al., 2012) and BRDT(1) (Morinière et al., 2009) peptide complexes that show both a primary and secondary Kac in a single binding pocket (and consistent with the stoichiometry observed by ITC), BRD9 binds with each of the two
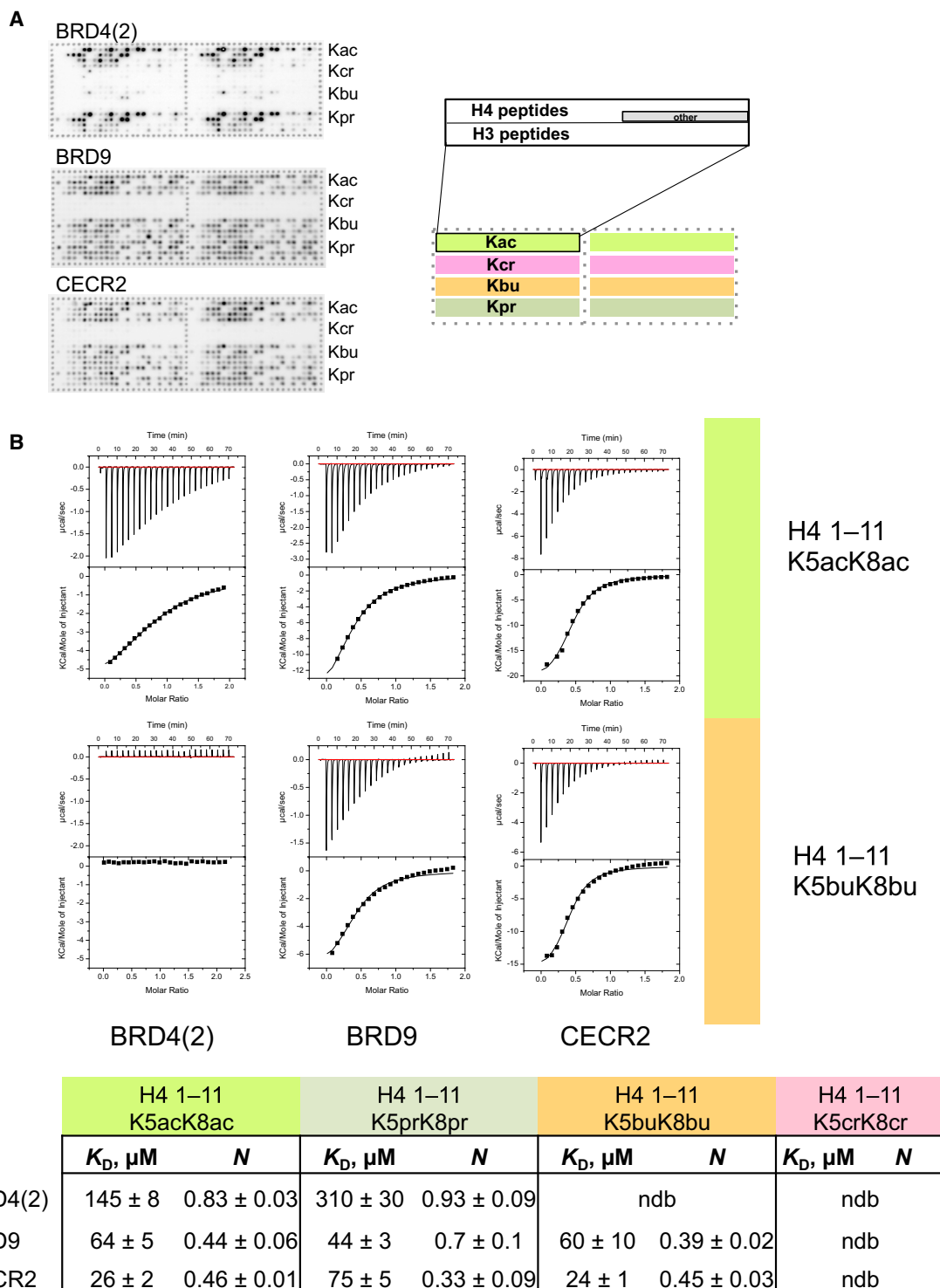
Figure 2. BRD9 and CECR2 Recognize Butyryllysine

(A) Binding of bromodomains to peptide arrays. Arrays include a series of 96 histone H3 and histone H4 peptides, each with one of four modification types, and are spotted in duplicate on left and right sides of the slide as indicated in the cartoon at right. See Table S1 for peptide sequences and a plate map. As previously reported (Vollmuth and Geyer, 2010), BRD4(2) is capable of binding to Kpr but does not recognize Kbu appreciably. In contrast, BRD9 and CECR2 are broadly capable of Kbu recognition (showing the same pattern as seen for the Kac peptides) but do not bind to Kcr.

(B) Solution binding constants and binding stoichiometry (*N*; peptide-to-bromodomain ratio) determined by isothermal titration calorimetry (ITC). A representative peptide, histone H4 residues 1–11, bearing two acetyl, two propionyl, or two butyryl modifications, was assessed for binding to the three bromodomains evaluated in (A). Note that BRD4(2) binds to only one acetyl group of the diacetylated H4 1–11 peptide per bromodomain-binding site, in contrast to the highly

(legend continued on next page)

	H4 1–11 K5acK8ac		H4 1–11 K5prK8pr		H4 1–11 K5buK8bu		H4 1–11 K5crK8cr	
	K_D, μM	*N*	K_D, μM	*N*	K_D, μM	*N*	K_D, μM	*N*
BRD4(2)	145 ± 8	0.83 ± 0.03	310 ± 30	0.93 ± 0.09	ndb		ndb	
BRD9	64 ± 5	0.44 ± 0.06	44 ± 3	0.7 ± 0.1	60 ± 10	0.39 ± 0.02	ndb	
CECR2	26 ± 2	0.46 ± 0.01	75 ± 5	0.33 ± 0.09	24 ± 1	0.45 ± 0.03	ndb	

modified peptide lysines occupying the primary binding site of a different bromodomain (Figure S2A). The inability to accommodate a second acetyl group in the binding site of BRD9 is consistent with the presence of a tyrosine gatekeeper: this feature has been associated with a "keyhole"-type pocket (Morinière et al., 2009) that can admit only a single acetyl group (Figure S2B). Thus, we obtained two views of the binding mode for each acylated peptide (BRD9 bound to either the K5acyl or K8acyl modification). In addition, we crystallized 1:1 complexes of BRD9 bound to each of the two sites of the Kbr and Kcr peptides (see Table 1). These structures show binding modes fully consistent with those seen in 2:1 complexes. The peptide tracks somewhat differently across the binding site in each K5/K8 comparison, but, importantly, the modified lysine side chains overlay closely (Figure S2C). Thus, for simplicity, further discussion centers on K5 acyl recognition unless otherwise noted.

As in the low-affinity H3K14bu-BRD4(1) complex (Vollmuth and Geyer, 2010), the conserved waters in the bottom of the pocket are well defined in the BRD9 Kbu complexes, and none is dislodged by ligand (Figure 3A). Despite this similarity, there are differences between the BRD9 and BRD4(1) Kbu complex structures that appear consistent with a higher-affinity interaction with the former bromodomain. Butyryllysine adopts a conformation in the BRD9-binding site that is well defined (Figure S4) but very different from that seen previously in the complex with BRD4(1) (Figure S3A). In the case of BRD4(1), the carbon chain of the butyryl group curls up from the bottom of the pocket, adopting a strained, eclipsed conformation with the terminal methyl group pointing toward the amide NH (Figures S3A and S3B). In contrast, the butyryl group in the BRD9 complex adopts a more favorable staggered conformation, and the butyryl group extends more fully into the binding pocket (Figures S3A, S3B, and S4). Overlay of the structures of BRD4(1) bound to Kac (Vollmuth et al., 2009) or Kbu (Vollmuth and Geyer, 2010) shows that the Kbu peptide is shifted slightly outward, and this results in repositioning of the butyryl carbonyl group relative to the asparagine anchor (Figure 3B). This carbonyl position may be less favorable, and, in combination with the associated strain evident in the ligand conformation, may account for the relatively poor affinities of BRD2 and BRD4 bromodomains for butyrylated peptides (Vollmuth and Geyer, 2010) (see also Figure 2B). In contrast, the Kbu modification is fully accommodated in the BRD9-binding site, and the butyryl carbonyl adopts a position very similar to that seen for a bound acetyl group (Figure 3C). It appears, therefore, that the BRD9-binding pocket may have greater flexibility than is typical.

Comparison of BRD9 structures with increasing size of acyl modification reveals how the binding site may adjust to the larger Kbu ligand. The bottom of the pocket is defined by the invariant phenylalanine residue of the "WPF shelf" motif (F45 in BRD9; see also Figure 1C). In the DMSO complex structure, the F45 side chain adopts a position pointing outward toward ligand. As the size of the acyl modification increases, the phenyl ring of F45

is deflected backward into the protein core to accommodate ligand (Figure 3D). Interestingly, no such movement of the analogous F83 is seen in comparison of apo (Lucas et al., 2013), Kac (Vollmuth et al., 2009), Kpr (Vollmuth and Geyer, 2010), and Kbu (Vollmuth and Geyer, 2010) complexes of BRD4(1) (Figure 3E), consistent with the more stringent acyl recognition preferences of BRD4. The mobility of BRD9 F45 reaches an apparent limit in the Kbu complex: there is very little additional deflection induced by bound Kcr, despite the more extended ligand conformation required by the *trans* double bond of the crotonyl group. Instead it appears that, to fit in the pocket, the crotonyl group is distorted from an optimal coplanar arrangement of the double bond and amide (Figures 3F, S3C, and S4). This limit to the size of the pocket may underlie the very low affinity of BRD9 for Kcr ligands, and provides a subtle means by which the butyryl and crotonyl modifications may be discriminated.

The Second Bromodomain of TAF1 Recognizes Crotonyllysine

In addition to BRD9 and CECR2 bromodomains, TAF1(2) scored as binding to butyryllysine modifications on arrays (Figure S1; Table S2). However, unlike BRD9 and CECR2, TAF1(2) and the very closely similar TAF1L(2) bound robustly to crotonyllysine peptides on arrays (Figure S1 and Table S2) and were the only bromodomains we screened to do so. To verify this, we quantified acyl peptide binding to TAF1(2) by ITC (Figure 4A). The Kcr peptide bound to TAF1(2) with high affinity. However, large shifts in thermodynamic parameters were observed for Kcr binding to TAF1(2) compared with other ligands (Table S3). In particular, the relatively small enthalpy change observed upon binding Kcr was augmented by a significant and favorable entropic contribution.

As it was not evident why TAF1(2) should be capable of both Kbu and Kcr recognition, we determined structures of this bromodomain in 2:1 complexes (same stoichiometry as the 2:1 BRD9 structures, see Figure S2A) with each peptide (Table 1), allowing two independent views of the modes of Kbu and Kcr binding (Figure S5A). Bound Kbu (Figure 4B) adopts a conformation very similar to that seen in the BRD9 complex structure (Figure 3A), with the butyryl group oriented toward the invariant phenylalanine (F1528). However, Kcr bound to TAF1(2) adopts a different and consistent (Figures 4C, 4D, and S5A) orientation in the pocket. The crotonyl group displaces two of the conserved, ordered water molecules from their usual positions (waters 3 and 4 as conventionally numbered; Hewings et al., 2012) (Figure 1C) and produces a significantly altered network of five rather than six waters (Figures 4C, 4D, and S5). Entry into the water pocket allows the crotonyl double bond to adopt a conformation more nearly coplanar with the Kcr amide than that seen in the BRD9 complex (dihedral angles defined by Nε and C1, C2, and C3 of the acyl chain of +166° versus −120° for TAF1(2) and BRD9 complexes, respectively; Figure S5B). The improved geometry of the Kcr group in the TAF1(2) complex is consistent with the observed higher-affinity interaction. Furthermore, the

---

similar BRD4(1) that accommodates two acetyl groups (Filippakopoulos et al., 2012; Morinière et al., 2009); see Figure S2B. BRD4(2) is therefore better suited to quantifying acyl recognition capacity in the primary site. Injection series for acetyl and butyryl peptides are shown at top and center, respectively. Fitted binding constants are shown in the table below, with average values and SEM based on at least three experiments per entry (see also Table S3). Note that the BRD7 bromodomain is highly similar to that of BRD9 and appeared to bind to Kbu in a manner similar to BRD9 (Table S2); however, the low solubility of BRD7 precluded confirmation of binding by ITC. See also Figure S2.

Table 1. Crystallization Conditions and Data Collection and Refinement Statistics for Crystal Structures

Structure	BRD9-DMSO	BRD9-KAc 2:1	BRD9-KBu 2:1	BRD9-KCr 2:1	BRD9-K5Bu	BRD9-K8Bu	BRD9-K5Cr	BRD9-K8Cr	TAF1(2)-Kbu 2:1	TAF1(2)- KCr 2:1
Ligand	DMSO	H4(1–11) K5ac/K8ac	H4(1–11) K5bu/K8bu	H4(1–11) K5cr/K8cr	H4(1–11) K5bu/K8bu	H4(1–11) K5bu/K8bu	H4(1–11) K5cr/K8cr	H4(1–11) K5cr/K8cr	H4(1–11) K5bu/K8bu	H4(1–11) K5cr/K8cr
Accession (PDB)	4YY4	4YYI	4YYJ	4YYK	4YY6	4YYG	4YYD	4YYH	4YYM	4YYN
Data Collection[a]										
Space group	C222$_1$	P1	P1	P1	C2	C222$_1$	C222$_1$	C2	P2$_1$2$_1$2$_1$	P2$_1$2$_1$2$_1$
Cell dimensions										
a, b, c (Å)	35.15, 68.55, 105.18	24.75, 34.60, 129.36	24.82, 34.33, 129.07	24.84, 34.73, 129.08	127.80, 35.07, 30.16	35.12, 69.83, 104.55	35.44, 71.02, 102.37	126.15, 35.70, 65.02	58.22, 66.05, 81.02	59.01, 66.00, 80.30
α, β, γ (°)	90.00, 90.00, 90.00	88.79, 90.00, 68.92	90.86, 90.00, 111.19	89.88, 89.81, 69.45	90.00, 92.32, 90.00	90.00, 90.00, 90.00	90.00, 90.00, 90.00	90.00, 99.01, 90.00	90.00, 90.00, 90.00	90.00, 90.00, 90.00
Resolution (Å)	50.00–1.47 (1.52–1.47)[b]	50.00–1.50 (1.55–1.50)	50.00–1.85 (1.92–1.85)	50.00–1.68 (1.74–1.68)	50.00–1.45 (1.50–1.45)	50.00–2.10	50.00–1.52 (1.57–1.52)	50.00–1.74 (1.80–1.74)	50.00–1.50 (1.55–1.50)	50.00–1.85 (1.85)
R$_{sym}$	0.052 (0.354)	0.052 (0.252)	0.080 (0.379)	0.095 (0.475)	0.074 (0.289)	0.062 (0.473)	0.037 (0.601)	0.043 (0.432)	0.048 (0.820)	0.052 (0.681)
I/σI	29.09 (3.11)	15.34 (3.14)	9.34 (2.00)	10.91 (1.96)	13.02 (3.06)	14.66 (1.81)	36.22 (2.99)	21.00 (2.26)	29.19 (1.75)	25.94 (2.35)
Completeness (%)	96.5 (80.8)	95.1 (94.0)	97.4 (95.5)	96.6 (99.9)	95.1 (70.3)	95.2 (83.5)	99.5 (98.7)	99.8 (100.0)	99.3 (97.7)	99.9 (100.0)
Redundancy	5.8 (4.9)	2.3 (2.3)	2.0 (1.9)	3.7 (3.1)	3.1 (2.0)	4.3 (4.0)	5.9 (5.6)	3.6 (3.7)	6.0 (5.3)	6.1 (6.1)
Refinement										
Resolution (Å)	50.00–1.47	50.00–1.50	50.00–1.85	50.00–1.80	50.00–1.45	50.00–2.10	50.00–1.52	50.00–1.74	50.00–1.50	50.00–1.85
No. of reflections	20,147	57,601	31,200	28,170	21,583	7,156	18,944	28,245	47,895	26,139
R$_{work}$/R$_{free}$	0.217/0.234	0.206/0.242	0.198/0.244	0.225/0.261	0.180/0.208	0.253/0.311	0.199/0.226	0.212/0.260	0.218/0.260	0.213/0.243
No. of atoms	929	3,639	3,512	3,467	1,049	858	1,040	1,925	2,433	2,295
Protein	825	815/815/821/ 821[c]	821/821/821/ 821	821/821/821/ 821	831	815	824	831/840	1,086/1,095	1,074/1,060
Ligand/ion	4 (DMSO)	40/40 (pep)	44/44 (pep)	44/44 (pep)	71 (pep)	22 (pep)	71 (pep)	26/26 (pep)	52/1 (pep/Ca)	77 (pep)
Water	100	287	140	95	147	21	145	202	199	84
B factors										
Protein	24.73	19.52/20.72/ 27.77/20.43[d]	16.45/17.11/ 18.39/18.68	26.82/25.05/ 24.06/25.02	13.64	29.09	21.32	24.69/25.75	21.36/25.31	27.86/29.27
Ligand/ion	33.72 (DMSO)	20.33/29.27 (pep)	28.22/30.18 (pep)	36.40/36.41 (pep)	46.06 (pep)	43.33 (pep)	49.84 (pep)	40.66/49.69 (pep)	42.79/23.18 (pep/Ca)	33.79 (pep)
Water	34.67	31.02	25.98	26.62	31.23	33.87	36.3	39.06	34.64	37.57
Root-mean-square deviations										
Bond lengths (Å)	0.032	0.028	0.019	0.028	0.026	0.016	0.023	0.022	0.022	0.02
Bond angles (°)	2.764	2.752	1.85	2.846	2.491	1.967	2.242	2.001	2.178	1.99

(Continued on next page)

Table 1. Continued

Structure	BRD9-DMSO	BRD9-KAc 2:1	BRD9-KBu 2:1	BRD9-KCr 2:1	BRD9-K5Bu	BRD9-K8Bu	BRD9-K5Cr	BRD9-K8Cr	TAF1(2)-Kbu 2:1	TAF1(2)-KCr 2:1
Ramachandran[e]										
Preferred	98 (98.99%)	395 (98.26%)	396 (98.02%)	376 (93.07%)	106 (98.15%)	97 (75.98%)	106 (99.07%)	203 (99.02%)	258 (99.23%)	247 (98.41%)
Allowed	1 (1.01%)	7 (1.74%)	8 (1.98%)	24 (5.94%)	2 (1.85%)	2 (2.02%)	1 (0.93%)	2 (0.98%)	2 (0.77%)	4 (1.59%)
Not allowed	0 (0.00%)	0 (0.00%)	0 (0.00%)	4 (0.99%)	0 (0.00%)	0 (0.00%)	0 (0.00%)	0 (0.00%)	0 (0.00%)	0 (0.00%)
Crystallization	0.1 M HEPES (pH 7.5); 25% w/v PEG 3350	0.1 M Bis-tris (pH 6.5); 25% w/v PEG 3350	0.2 M NH₄Cl; 20% w/v PEG 3350	0.1 M MES (pH 6.5); 15% w/v PEG 550 MME	0.2 M Na malonate (pH 4.0); 20% w/v PEG 3350	0.05 M CaCl₂ dihydrate; 0.1 M Bis-tris (pH 6.5); 30% v/v PEG MME 550	0.2 M Na malonate (pH 7.0); 20% w/v PEG 3350	0.1 M Na citrate (pH 5.5); 0.2 M NaCl; 20% w/v PEG 3350	0.2 M CaCl₂; 20 w/v PEG 3350	0.2 M Ca acetate; 20% w/v PEG 3350

[a]A single crystal was used to collect data for each of the structures reported here.
[b]Values in parentheses are for highest-resolution shell.
[c]Where multiple chains exist for the protein/peptide complexes, the atom numbers were listed for the individual polypeptide chains separated by "/", where "pep" stands for peptide.
[d]Where multiple chains exist for the protein/peptide complexes, the B factors were listed for the individual polypeptide chains separated by "/", where "pep" stands for peptide.
[e]Number of residues (percentage).

net displacement of one water molecule may contribute to the favorable entropy change upon Kcr binding (Table S3).

Defining Determinants for and Reengineering Butyryllysine Specificity

Although some bromodomains proved capable of robust butyryl- and crotonyllysine recognition, we were surprised there were not more examples. Our hypothesis was that bromodomains with non-β-branched gatekeepers might have expanded acyl recognition capacity, and indeed BRD7/9, CECR2, and TAF1(2)/TAF1L(2) (of SGC structural classes IV, I, and VII, respectively; Filippakopoulos et al., 2012), with tyrosine gatekeepers (Figure 5A), fall into this group. However, there are other bromodomains with aromatic gatekeepers (Figure 5A) that do not bind appreciably to Kbu on arrays: class I bromodomains GCN5, PCAF, and BPTF, and class IV bromodomains BRPF1, BRD1, and BRPF3. (However, note that GCN5 and PCAF bind poorly even to acetylated peptides on arrays [Table S2].) Taken together, an aromatic gatekeeper is necessary for Kbu recognition but not sufficient. In examining the structures of BRD9 and the deflecting F45 (Figure 3D), it appeared that a methionine residue (M92) in the protein core behind F45 might aid in its mobility and, along with the tyrosine gatekeeper, create a larger binding pocket. The equivalent residue in CECR2 (position 506) is also methionine, while in other bromodomains it is often a more rigid β-branched residue (isoleucine in the BRPF family and valine in GCN5/PCAF; see Figure 5A). Interestingly, in the BET-class bromodomains, which do not bind Kbu with high affinity (Vollmuth and Geyer, 2010) (Figure 2B), the equivalent residue is invariably methionine, but the BET-class bromodomains are encumbered with a β-branched gatekeeper residue.

To explore whether the tyrosine gatekeeper and core methionine were required for Kbu recognition, we mutated these residues to isoleucine in CECR2 and BRD9. Importantly, these mutants retain full affinity for the Kac peptide (Figure 5B) and have thermal stabilities comparable to those of the wild-type bromodomains (Table S4). However, mutation of either residue in BRD9 or in CECR2 resulted in the loss of any detectable binding to the Kbu peptide (Figure 5B). This suggests that restriction of the binding pocket by a β-branched gatekeeper or a relatively rigid protein core can each contribute to selectivity for Kac. However, the system is not entirely modular: consistent with a previous report (Morinière et al., 2009), substituting tyrosine for the isoleucine gatekeeper in BET-class bromodomains did not confer any expanded acyl recognition capacity despite the presence of the core methionine, nor did we find any case in which introducing a core methionine in the presence of a permissive gatekeeper (for example, into the BRPF family) resulted in a gain of Kbu binding (not shown).

Given our inability to engineer novel Kbu binding in the initial round of mutagenesis, we sought additional features that might govern ligand specificity. The "WPF shelf" region of the ZA loop contributes to one side of the ligand-binding pocket. In the class IV bromodomains (Figure 5A), the canonical WPF motif is replaced by GFF (BRD9) or XIF (BRPF family). BRPF1 I652 appears to restrict this side of the binding pocket compared with F44 of BRD9 (Figure 6A, right). Accordingly, we evaluated I-to-F mutants across the family (BRPF1, BRD1, BRPF3). Screening of the mutants on peptide arrays showed a general gain in Kbu
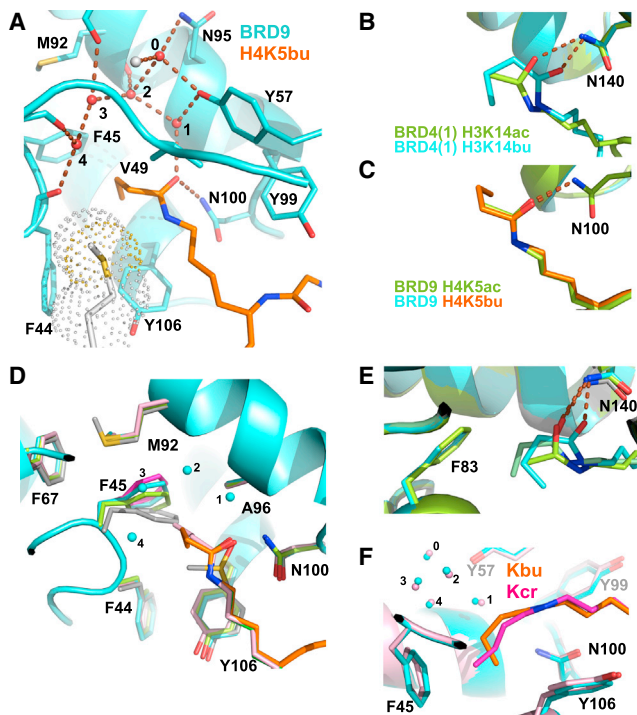
Figure 3. Acyllysine Recognition by BRD9

(A) H4K5bu (orange) bound to BRD9. The butyryl carbonyl (top) forms the expected hydrogen bond to N100 (the anchor). Y106 is the gatekeeper residue discussed in the text. The small numbered spheres indicate ordered waters (see Figure 1C); these form a network of hydrogen bonds with backbone carbonyls of M92 (water 2), M65 (waters 3), F47 (water 4), and F44 (water 4), the side chains of Y57 and N95, and the ligand acyl oxygen. The methionine side chain shown in dot representation (M59) is from an adjacent BRD9 monomer in the crystal, and packs against a shallow cleft formed by side chains of F44 and Y106 and the ligand (near Nε and C2 but not close to C3 or C4). The small white sphere (unnumbered) is water −1 (see Figure 1C). Note that for consistency with entry PDB: 3HME, residue numbering is that of isoform 3 (UniProt: Q9H8M2-3) rather than that of isoform 1 (UniProt: Q9H8M2-5).

(B and C) Comparison of Kbu binding to BRD4(1) and BRD9. Kac and Kbu complexes are overlaid. (B) For BRD4, the Kbu interaction is of very low affinity, and the acyl group (cyan; PDB: 3MUL; Vollmuth and Geyer, 2010) is shifted in the binding site relative to the position of Kac (green; PDB: 3JVK; Vollmuth et al., 2009). Although not shown for clarity, the two protein structures overlay closely and exhibit no significant side-chain rearrangements. (C) For BRD9, Kbu ligand (orange) occupies a position similar to that of Kac ligand (green), and overlaid proteins show no significant differences in the binding pocket other than that shown in (D).

(D) BRD9 bound to ligands of increasing size. Structures in complex with DMSO (gray), Kac (green), Kbu (orange), and Kcr (pink) are overlaid. With the exception of BRD9 (cyan) in the Kbu complex, bromodomain residues are colored to match ligand. The F45 phenyl ring deflects back into the protein core as ligand size increases, but this appears to reach nearly its maximum extent in the Kbu complex: there is little additional movement apparent in the very low-affinity Kcr complex. Note that the view is clipped in front so that F45 can be seen clearly.

(E) Overlaid structures of BRD4(1) in apo form or bound to ligands of increasing size show that F83 (analogous to BRD9 F45) does not move to accommodate ligand. Structures (in addition to those shown in B) are apo (gray; PDB: 4LYI; Lucas et al., 2013) and Kpr-bound (darker green; PDB: 3MUK; Vollmuth and Geyer, 2010).

(F) Low-affinity Kcr binding to BRD9 is accommodated by structural deformation of the ligand. A different view (relative to D) of bound Kbu (orange) and Kcr (pink) shows the well-accommodated conformation of the butyryl group. The *trans* double bond of the crotonyl group precludes the ligand adopting

binding (Figures 6A and S6). For wild-type and mutant BRD1, we quantified binding by ITC (Figure 6B). Importantly, the mutation does not impair Kac binding yet allows equally potent recognition of a new mark, Kbu. Like CECR2 and BRD9, I586F mutant BRD1 discriminates against Kcr (Figure 6A).
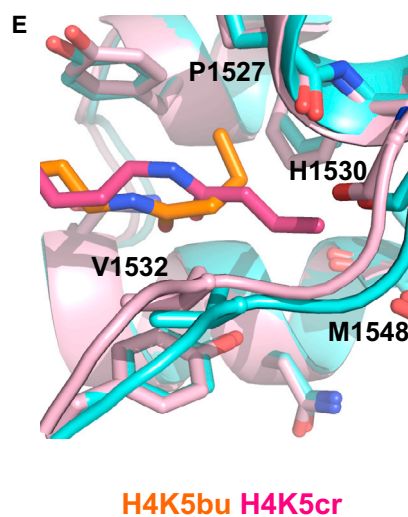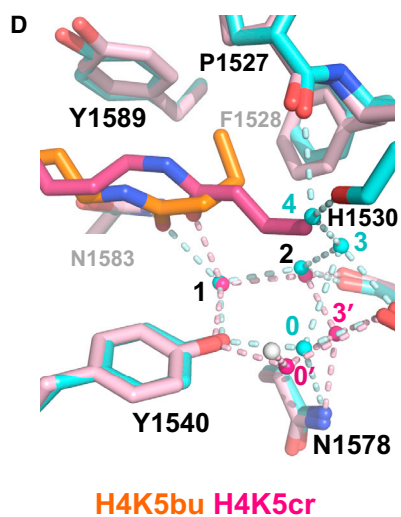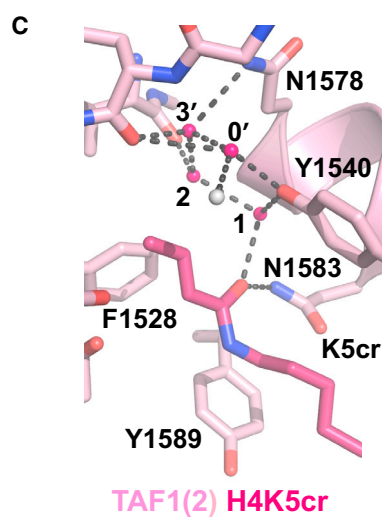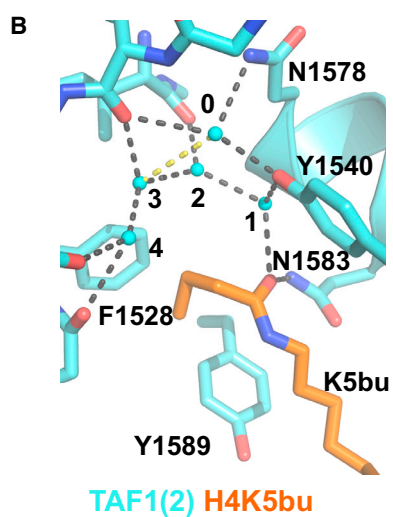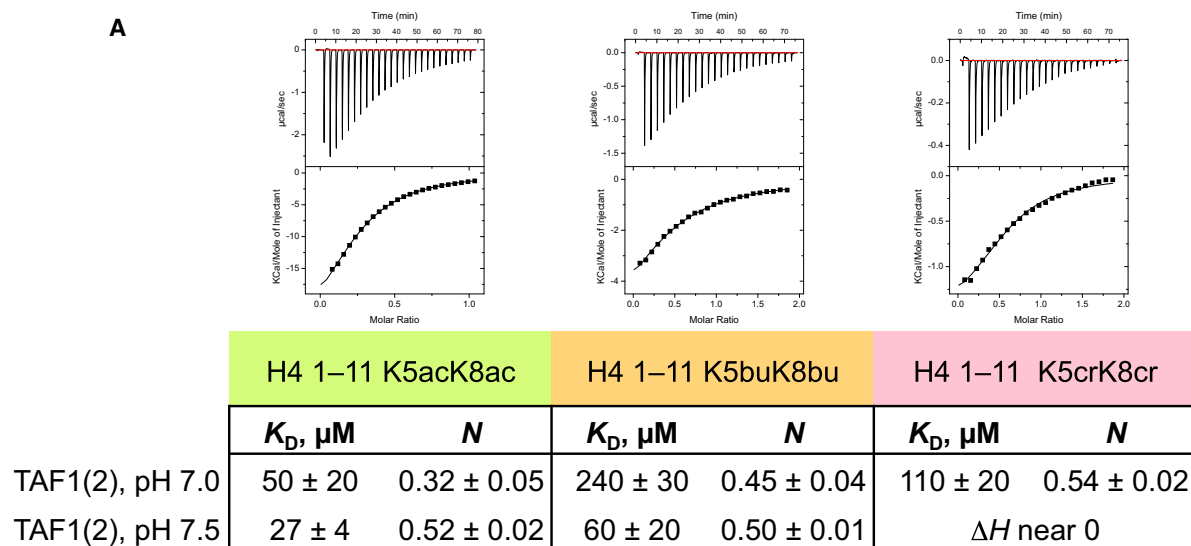
DISCUSSION

Lysine acetylation is an integrator of information on metabolic status (Gut and Verdin, 2013; Lu and Thompson, 2012; Xing and Poirier, 2012; Zhao et al., 2010), especially in mitochondria (Amado et al., 2014; Newman et al., 2012), circadian rhythms (Masri et al., 2013), cellular environment (McBrian et al., 2013), and signal transduction pathways (Bannister and Miska, 2000; Choudhary et al., 2009; Shahbazian and Grunstein, 2007). Efforts to catalog the "acetylome" have revealed that, in addition to histones, many non-histone proteins are modified (Choudhary et al., 2009; Kaluarachchi Duffy et al., 2012; Weinert et al., 2011). Indeed, the scope and potential importance of acetylation biology has been equated to that of phosphorylation (Kouzarides, 2000; Norris et al., 2009; Smith and Workman, 2009). Acetylation status can be interpreted in a number of ways, including regulation of enzymatic activity, direct changes in chromatin structure, or localization of protein complexes to histones through bromodomain proteins. Accordingly, bromodomains and other acetyllysine readers (Li et al., 2014; Zeng et al., 2010) are often found in proteins that function in transcriptional regulation and chromatin remodeling. The investigation of bromodomains has advanced by use of selective, cell-permeable small-molecule inhibitors (chemical probes) that compete with acetyllysine for binding to the bromodomain, and thereby disrupt its function within larger proteins and complexes (Chung, 2012; Filippakopoulos and Knapp, 2014; Hewings et al., 2012; Sanchez et al., 2014). In the case of BET-class bromodomains, such studies have revealed profound biological effects, propelling BET inhibitors into clinical studies (Dawson et al., 2012; Shi and Vakoc, 2014).
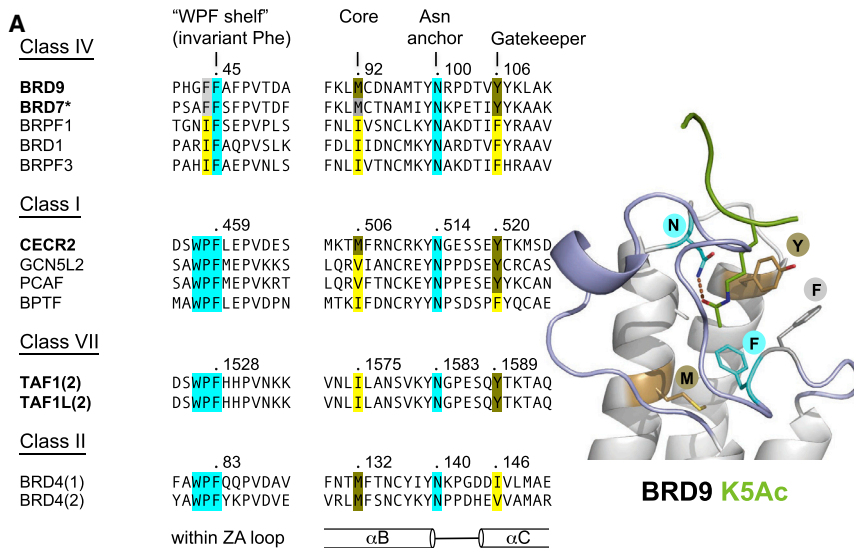
In this study, we establish that a small number of human bromodomains, those of TAF1, CECR2, and BRD9 (and presumably also those of the closely related TAF1L and BRD7) are capable of reading crotonyl or butyryl marks on histone peptides with affinities comparable to their affinities for acetyl modifications. This suggests that such binding could be physiologically meaningful and potentially function in chromatin regulation. It is interesting that, even for those bromodomains capable of recognizing larger acyl groups, we found no preferential binding to these marks over acetyl. Finally, we found that no bromodomain is capable of recognizing succinyl modifications, and only the non-canonical bromodomain PHIP(2) appears to bind formyl modifications in histone peptides (Figure S1). Formyllysine may be the consequence of oxidative damage (Edrissi et al., 2013; Jiang et al., 2007) rather than a regulated mark, perhaps explaining why it

such a conformation, and instead the double bond twists out of the plane of the amide group (see also Figure S3C). In both structures, the six ordered water molecules described in (A) and the text (five of these shown as small spheres) remain largely in place, although electron density is weak for select examples (see Figure S2C).

See also Figures S2, S3, and S4.

A

	H4 1–11 K5acK8ac		H4 1–11 K5buK8bu		H4 1–11 K5crK8cr	
	K_D, μM	N	K_D, μM	N	K_D, μM	N
TAF1(2), pH 7.0	50 ± 20	0.32 ± 0.05	240 ± 30	0.45 ± 0.04	110 ± 20	0.54 ± 0.02
TAF1(2), pH 7.5	27 ± 4	0.52 ± 0.02	60 ± 20	0.50 ± 0.01	ΔH near 0	

(legend on next page)

A

| | "WPF shelf" (invariant Phe) | Core | Asn anchor | Gatekeeper |

Class IV

	.45	.92	.100	.106
BRD9	PHGFFAFPVTDA	FKLMCDNAMTYNRPDTVYYKLAK
BRD7*	PSAFFSFPVTDF	FKLMCTNAMIYNKPETIYYKAAK
BRPF1	TGNIFSEPVPLS	FNLIVSNCLKYNAKDTIFYRAAV
BRD1	PARIFAQPVSLK	FDLIIDNCMKYNARDTVFYRAAV
BRPF3	PAHIFAEPVNLS	FNLIVTNCMKYNAKDTIFHRAAV

Class I

	.459	.506	.514	.520
CECR2	DSWPFLEPVDES	MKTMFRNCRKYNGESSEYTKMSD
GCN5L2	SAWPFMEPVKKS	LQRVIANCREYNPPDSEYCRCAS
PCAF	SAWPFMEPVKRT	LQRVFTNCKEYNPPESEYYKCAN
BPTF	MAWPFLEPVDPN	MTKIFDNCRYYNPSDSPFYQCAE

Class VII

	.1528	.1575	.1583	.1589
TAF1(2)	DSWPFHHPVNKK	VNLILANSVKYNGPESQYTKTAQ
TAF1L(2)	DSWPFHHPVNKK	VNLILANSVKYNGPESQYTKTAQ

Class II

	.83	.132	.140	.146
BRD4(1)	FAWPFQQPVDAV	FNTMFTNCYIYNKPGDDIVLMAE
BRD4(2)	YAWPFYKPVDVE	VRLMFSNCYKYNPPDHEVVAMAR

within ZA loop   αB   αC

BRD9 K5Ac

Figure 5. Acyl Selectivity Determinants in Bromodomains

(A) Aligned partial sequences of bromodomains showing positions of key features. Residue numbers correspond to the residue marked by a dot in the top sequence of each class. Names are shown in bold for bromodomains capable of butyryllysine recognition (*see note for BRD7 in legend of Figure 2). Invariant or very common features are highlighted in cyan, while more variable features targeted by mutagenesis are highlighted in yellow, brown, or gray. The cartoon on the right (BRD9) includes specific side chains discussed in the text labeled with circles and color coded to BRD9 in the alignment. See Figure 1B for additional labeling of features.

(B) Kbu recognition by BRD9 and CECR2 requires a permissive tyrosine gatekeeper and a core methionine residue. ITC results for wild-type and mutant BRD9 and CECR2. Fitted values are averages and SEM from at least three ITC experiments per entry (see also Table S3).

B

	H4 1–11 K5acK8ac		H4 1–11 K5buK8bu	
	K_D, μM	N	K_D, μM	N
BRD9 wt	64 ± 5	0.44 ± 0.06	60 ± 10	0.39 ± 0.02
Y106I	60 ± 10	0.51 ± 0.04		ndb
M92I	25 ± 2	0.5 ± 0.1		ndb
CECR2 wt	26 ± 2	0.46 ± 0.01	24 ± 1	0.45 ± 0.03
Y520I	32 ± 2	0.44 ± 0.02		ndb
M506I	17.3 ± 0.4	0.46 ± 0.01		ndb

Mutagenesis of BRD9 and CECR2 identified two residues as critical in allowing high-affinity recognition of butyryllysine: a tyrosine gatekeeper and a core methionine. However, while an aromatic gatekeeper appeared to be required, it was not sufficient to support Kbu binding, and, in the case of TAF1(2), Kbu bound with substantial (if not full) affinity despite TAF1(2) lacking the core methionine residue. Likewise, introduction of these residues into Kac-specific bromodomains did not yield mutants with broader recognition properties. In the case of BRD1 and other BRPF family bromodomains, a residue substitution at a third site (in the "WPF shelf" region) was instead sufficient to recruit novel butyryllysine recognition. As in the case of TAF1(2), this was possible despite the presence in the BRPF family of the core isoleucine residue that, when introduced into BRD9 or

is not recognized by canonical bromodomains or HDACs (Edrissi et al., 2013). In contrast, succinyllysine appears to be an evolutionarily conserved mark (Weinert et al., 2013; Xie et al., 2012) with a dedicated, carboxyl-specific deacetylase, SIRT5 (Du et al., 2011; Park et al., 2013; Peng et al., 2011; Tan et al., 2014). It will be interesting to explore whether another class of proteins may read succinyllysine or similar acidic modifications.

Figure 4. TAF1(2) Is Competent to Read Crotonyllysine

(A) Evaluation of Kac, Kbu, and Kcr binding to TAF1(2) by ITC. Measurements were made at pH 7.0 in addition to pH 7.5 (see Experimental Procedures). In each case, the traces shown are representative of pH 7.0 data. Average values and SEM are based on three measurements for Kac and Kbu peptides at each condition and seven measurements for the Kcr peptide at pH 7.0 (Table S3).

(B) Kbu peptide bound to TAF1(2). The K5 modification is shown, and the binding mode appears equivalent to that of K8bu (Figure S4A). Note similarity of ligand conformation to that shown in Figure 3A and the presence of five ordered water molecules (the sixth, water −1, is not shown to avoid obscuring other details). In the case of TAF1, water 0 appears slightly closer to water 3 (yellow dotted line) than to water 2 (as in BRD9 complexes). The four unlabeled backbone carbonyls in the upper left part of the image are from I1575, M1548, H1530, and P1527, shown interacting with waters 2, 3, 4, and 4, respectively.

(C) Kcr peptide bound to TAF1(2). The orientation is the same as in (B) and shows the crotonyl group extending further into the pocket than does the butyryl group in (B). Note that two water molecules (numbers 3 and 4) have been displaced by ligand. A new, shifted network has formed in which the original water 0 is replaced by waters 0′ and 3′ (so designated because they form connections similar to waters 0 and 3; see text and D). The white sphere is water −1 (see Figure 1C).

(D) Overlay of Kcr and Kbu TAF1(2) complexes reoriented to highlight the different binding modes of the acyl carbon chains and details of the rearranged water networks. The color scheme is the same as in (B) and (C). H1530 is not shown for the Kcr complex so that the interaction between water 4 and H1530 in the Kbu complex may be seen. The unlabeled backbone carbonyls on the right are those of I1575 and M1548, interacting with waters 2 and 0, 3 (or 0′, 3′ for Kcr complex), respectively. As noted above, water 3′ shows connectivity related to that of canonical water 3 (water 2, water 0, H1530). However, it is located ∼3 Å from the position of water 3 in the Kbu complex and much closer to N1578. Water 0′ shifts ∼1.2 Å from the position of water 0 and further away from N1578 (see also C).

(E) Additional interactions of TAF1(2) with the crotonyl group. The side chain of V1532 and the carbonyls of P1527, H1530, and M1548 (each carbonyl normally interacts with water 3 or 4) point toward the crotonyl group and pack loosely. Unlike the butyryl group in the Kbu complex, there is little packing of the crotonyl group with F1528. The waters are omitted from this panel for clarity.
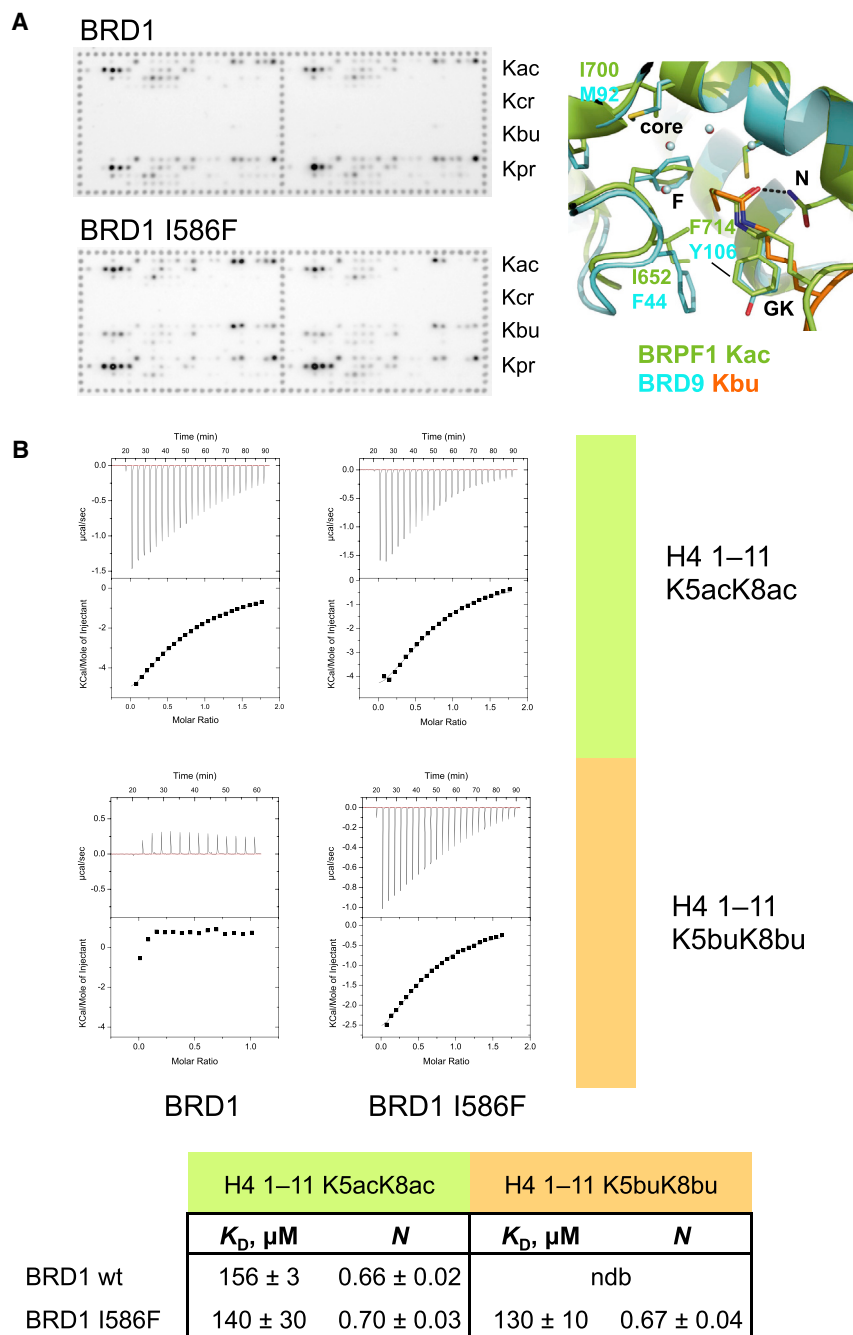
See also Figures S4 and S5.

A

BRD1

Kac
Kcr
Kbu
Kpr

BRD1 I586F

Kac
Kcr
Kbu
Kpr

Figure 6. Gain of Kbu Recognition in a ZA Loop Mutant of BRD1

(A) Left: Binding of BRD1 wild-type and mutant assessed by peptide array. Wild-type bromodomain shows no appreciable recognition of Kbu peptides, whereas significant binding is evident for the I586F mutant. Right: Overlay of BRD9 and BRPF1 peptide complexes (PDB: 4QYD; Lubula et al., 2014) showing proximity of the site of mutation and bound ligand. Key differences between BRD9 and BRPF1 are indicated in color-coded labels (these three residues are identical in BRD1 and BRPF1; BRD1 numbering is I586, I634, and F648). Black labels relate to features shown in Figure 5A.

(B) ITC assessment of the acyl specificity change indicated by data shown in (A). Reported values are averages and SEM based on three ITC experiments per entry (Table S3).

See also Figure S6.

B

H4 1–11
K5acK8ac

H4 1–11
K5buK8bu

BRD1   BRD1 I586F

	H4 1–11 K5acK8ac		H4 1–11 K5buK8bu	
	K_D, µM	N	K_D, µM	N
BRD1 wt	156 ± 3	0.66 ± 0.02	ndb	
BRD1 I586F	140 ± 30	0.70 ± 0.03	130 ± 10	0.67 ± 0.04

unsaturated crotonyl group, which is therefore excluded. In the case of TAF1(2) an alternative is available, namely displacement of conserved waters in the base of the pocket by a reoriented crotonyl group. It is not presently clear why water displacement is possible for TAF1(2) but not for BRD9 (nor, presumably, CECR2). In any case, the discrimination of butyryl and crotonyl modifications by CECR2 and BRD9 is remarkable, and suggests that these histone marks could have distinct physiological functions.

The expansion of the histone acyllysine repertoire to include a broad range of modifications beyond acetyl is provocative and suggests a more nuanced view of cellular response to metabolic status at the level of chromatin. However, these non-acetyl modifications are considerably less abundant than acetyllysine, and may be largely restricted to particular tissues (Tan et al., 2011) or limited to a narrower range of histone lysines than the acetyl mark. Accordingly, although associations have been drawn between genomic locations of these marks and possible functions (Dai et al., 2014; Tan et al., 2011; Wisniewski et al., 2008; Xie et al., 2012), there is little information available about what the specific consequences of these modifications (or their loss) might be. One possibility is that a non-acetyl modification could compete with acetylation at a particular site and thereby antagonize recruitment of an acetyl-specific reader. On the other hand, a non-acetyl modification might partially mimic the direct effect of acetylation on chromatin structure, as it would be capable of neutralizing positive charge on histone tails in the same way as acetylation and thereby decompact chromatin. An exciting possibility is that non-acetyl acyllysine marks lead to defined changes in transcriptional status based on a

CECR2, abolished Kbu recognition. It would seem, therefore, that bromodomain acyl ligand recognition and specificity are complex. Nevertheless, it appears that rather simple changes in the bromodomain can lead to gain of new binding function, and that the high specificity that most bromodomains show for Kac may be under active selection.

The structures we report illustrate further both the plasticity of the bromodomain binding site and its subtlety. High-affinity butyryllysine recognition appears to require deformation in the protein core to accommodate the acyl carbon chain in a particular bent conformation. This conformation is not achievable by the

difference in the complexes recruited to such sites. This would provide a new means of response to changes in the proportion of acyl-CoAs in the cell (Newman et al., 2012), allowing fine-tuning of transcriptional response to metabolic status (Eckel-Mahan et al., 2012; Masri et al., 2012). The identification of reader domains capable of interpreting non-acetyl acyl marks is a key step in establishing the potential of this latter mechanism.

EXPERIMENTAL PROCEDURES

Bromodomain Protein Production

Bromodomains were expressed in *Escherichia coli* and purified by a combination of affinity and conventional chromatography methods. Details are given in the Supplemental Experimental Procedures. Full details of the constructs used (DNA sequence, tagging scheme, resulting expressed protein, and amino acid boundaries within the full-length protein) are given in Table S5.

Synthesis of Peptides and Peptide Arrays

Peptides were synthesized by standard solid-phase Fmoc chemistry (Anaspec). Peptides for arrays were custom synthesized in 384-well format using CelluSpots technology and spotted on slides for binding studies (Intavis Peptide Services). Fmoc-acyllysines not commercially available were synthesized as described in the Supplemental Experimental Procedures. See also Table S1 for peptide sequences.

Screening of Bromodomain Binding to Peptide Arrays

Peptide arrays were incubated with 25 μM bromodomain solution overnight at 4°C. Bound bromodomain was detected through the FLAG tag (α-FLAG M2 HRP conjugate) as described in Supplemental Experimental Procedures. See also Table S2.

Measurement of Peptide Dissociation Constants by ITC

Experiments were carried out on an ITC200 (MicroCal). Typically, 200–400 μM protein was placed in the calorimeter cell and peptide at a 10-fold higher concentration (2000–4000 μM) was injected into the cell. All experiments were performed at 25°C (298 K) in 20 mM HEPES (pH 7.5) and 150 mM NaCl, except those conducted at pH 7.0 as noted for TAF1(2). The enthalpy change for binding of the Kcr peptide to TAF1(2) at pH 7.5 is too close to zero to allow K_D determination by this method (Becktel and Schellman, 1987) provide a rationale for use of pH change to shift thermodynamic parameters. Measured affinities for Kac and Kbu peptides shift only 2- to 4-fold with the shift in pH, and binding of TAF1(2) to arrays appears similar at these pH values (not shown). Thermodynamic parameters were fitted in the MicroCal Origin software package using a single-site model, and are reported in detail in Table S3.

Crystallization and Structure Determination

Peptide complexes of BRD9 and TAF1(2) bromodomains were crystallized as described in Supplemental Experimental Procedures (see also Table 1 for specific conditions). Complete diffraction datasets for the protein-peptide complex crystals were collected either at the SER-CAT beamline at the Advanced Photon Source or the CMCF beamline at the Canadian Light Source. The data were processed and scaled with the HKL3000 program suite (Minor et al., 2006). The structures were solved by molecular replacement with 3HME (BRD9) or 1EQF (TAF1) as search models using Phaser in the CCP4 suite (McCoy et al., 2007; Potterton et al., 2002), and were refined using REFMAC5 (Winn et al., 2003) built into the Coot program (Emsley and Cowtan, 2004). Peptides were built onto the $2F_o$-F_c and F_o-F_c maps at the final stage of the refinement. Structures are validated using the built-in tools in Coot, as well as with PROCHECK (Laskowski et al., 1993) and MolProbity (Chen et al., 2010). Crystallographic data and refinement statistics of the individual structures are summarized in Table 1.

ACCESSION NUMBERS

Accession numbers for the structures reported in this paper are PDB: 4YY4, 4YYI, 4YYJ, 4YYK, 4YY6, 4YYG, 4YYD, 4YYH, 4YYM, and 4YYN.

SUPPLEMENTAL INFORMATION

Supplemental Information includes Supplemental Experimental Procedures, six figures, and five tables and can be found with this article online at http://dx.doi.org/10.1016/j.str.2015.08.004.

REFERENCES

Amado, F.M., Barros, A., Azevedo, A.L., Vitorino, R., and Ferreira, R. (2014). An integrated perspective and functional impact of the mitochondrial acetylome. Expert Rev. Proteomics *11*, 383–394.

Arnaudo, A.M., and Garcia, B.A. (2013). Proteomic characterization of novel histone post-translational modifications. Epigenetics Chromatin *6*, 24.

Bannister, A.J., and Miska, E.A. (2000). Regulation of gene expression by transcription factor acetylation. Cell Mol. Life Sci. *57*, 1184–1192.

Bao, X., Wang, Y., Li, X., Li, X.M., Liu, Z., Yang, T., Wong, C.F., Zhang, J., Hao, Q., and Li, X.D. (2014). Identification of 'erasers' for lysine crotonylated histone marks using a chemical proteomics approach. eLIFE *3*, e02999.

Becktel, W.J., and Schellman, J.A. (1987). Protein stability curves. Biopolymers *26*, 1859–1877.

Chen, Y., Sprung, R., Tang, Y., Ball, H., Sangras, B., Kim, S.C., Falck, J.R., Peng, J., Gu, W., and Zhao, Y. (2007). Lysine propionylation and butyrylation are novel post-translational modifications in histones. Mol. Cell Proteomics *6*, 812–819.

Chen, V.B., Arendall, W.B., 3rd, Headd, J.J., Keedy, D.A., Immormino, R.M., Kapral, G.J., Murray, L.W., Richardson, J.S., and Richardson, D.C. (2010). MolProbity: all-atom structure validation for macromolecular crystallography. Acta Crystallogr. D Biol. Crystallogr. *66*, 12–21.

Choudhary, C., Kumar, C., Gnad, F., Nielsen, M.L., Rehman, M., Walther, T.C., Olsen, J.V., and Mann, M. (2009). Lysine acetylation targets protein complexes and co-regulates major cellular functions. Science *325*, 834–840.

Chung, C.W. (2012). Small molecule bromodomain inhibitors: extending the druggable genome. Prog. Med. Chem. *51*, 1–55.

Chung, C.W., Coste, H., White, J.H., Mirguet, O., Wilde, J., Gosmini, R.L., Delves, C., Magny, S.M., Woodward, R., Hughes, S.A., et al. (2011). Discovery and characterization of small molecule inhibitors of the BET family bromodomains. J. Med. Chem. *54*, 3827–3838.

Dai, L., Peng, C., Montellier, E., Lu, Z., Chen, Y., Ishii, H., Debernardi, A., Buchou, T., Rousseaux, S., Jin, F., et al. (2014). Lysine 2-hydroxyisobutyrylation is a widely distributed active histone mark. Nat. Chem. Biol. *10*, 365–370.

Dawson, M.A., Kouzarides, T., and Huntly, B.J. (2012). Targeting epigenetic readers in cancer. N. Engl. J. Med. *367*, 647–657.

Dhalluin, C., Carlson, J.E., Zeng, L., He, C., Aggarwal, A.K., and Zhou, M.M. (1999). Structure and ligand of a histone acetyltransferase bromodomain. Nature *399*, 491–496.

Du, J., Zhou, Y., Su, X., Yu, J.J., Khan, S., Jiang, H., Kim, J., Woo, J., Kim, J.H., Choi, B.H., et al. (2011). Sirt5 is a NAD-dependent protein lysine demalonylase and desuccinylase. Science *334*, 806–809.

Eckel-Mahan, K.L., Patel, V.R., Mohney, R.P., Vignola, K.S., Baldi, P., and Sassone-Corsi, P. (2012). Coordination of the transcriptome and metabolome by the circadian clock. Proc. Natl. Acad. Sci. USA *109*, 5541–5546.

Edrissi, B., Taghizadeh, K., and Dedon, P.C. (2013). Quantitative analysis of histone modifications: formaldehyde is a source of pathological n(6)-formylly-sine that is refractory to histone deacetylases. PLoS Genet. *9*, e1003328.

Emsley, P., and Cowtan, K. (2004). Coot: model-building tools for molecular graphics. Acta Crystallogr. D Biol. Crystallogr. *60*, 2126–2132.

Feldman, J.L., Baeza, J., and Denu, J.M. (2013). Activation of the protein de-acetylase SIRT6 by long-chain fatty acids and widespread deacylation by mammalian sirtuins. J. Biol. Chem. *288*, 31350–31356.

Filippakopoulos, P., and Knapp, S. (2014). Targeting bromodomains: epige-netic readers of lysine acetylation. Nat. Rev. Drug Discov. *13*, 337–356.

Filippakopoulos, P., Picaud, S., Mangos, M., Keates, T., Lambert, J.P., Barsyte-Lovejoy, D., Felletar, I., Volkmer, R., Muller, S., Pawson, T., et al. (2012). Histone recognition and large-scale structural analysis of the human bromodomain family. Cell *149*, 214–231.

Furdas, S.D., Kannan, S., Sippl, W., and Jung, M. (2012). Small molecule inhib-itors of histone acetyltransferases as epigenetic tools and drug candidates. Arch. Pharm. (Weinheim) *345*, 7–21.

Garrity, J., Gardner, J.G., Hawse, W., Wolberger, C., and Escalante-Semerena, J.C. (2007). N-lysine propionylation controls the activity of pro-pionyl-CoA synthetase. J. Biol. Chem. *282*, 30239–30245.

Gattner, M.J., Vrabel, M., and Carell, T. (2013). Synthesis of epsilon-N-pro-pionyl-, epsilon-N-butyryl-, and epsilon-N-crotonyl-lysine containing histone H3 using the pyrrolysine system. Chem. Commun. (Camb) *49*, 379–381.

Gut, P., and Verdin, E. (2013). The nexus of chromatin regulation and interme-diary metabolism. Nature *502*, 489–498.

Haynes, S.R., Dollard, C., Winston, F., Beck, S., Trowsdale, J., and Dawid, I.B. (1992). The bromodomain: a conserved sequence found in human, *Drosophila* and yeast proteins. Nucleic Acids Res. *20*, 2603.

Hewings, D.S., Rooney, T.P., Jennings, L.E., Hay, D.A., Schofield, C.J., Brennan, P.E., Knapp, S., and Conway, S.J. (2012). Progress in the develop-ment and application of small molecule inhibitors of bromodomain-acetyl-lysine interactions. J. Med. Chem. *55*, 9393–9413.

Jiang, T., Zhou, X., Taghizadeh, K., Dong, M., and Dedon, P.C. (2007). N-for-mylation of lysine in histone proteins as a secondary modification arising from oxidative DNA damage. Proc. Natl. Acad. Sci. USA *104*, 60–65.

Jiang, H., Khan, S., Wang, Y., Charron, G., He, B., Sebastian, C., Du, J., Kim, R., Ge, E., Mostoslavsky, R., et al. (2013). SIRT6 regulates TNF-alpha secretion through hydrolysis of long-chain fatty acyl lysine. Nature *496*, 110–113.

Kaluarachchi Duffy, S., Friesen, H., Baryshnikova, A., Lambert, J.P., Chong, Y.T., Figeys, D., and Andrews, B. (2012). Exploring the yeast acetylome using functional genomics. Cell *149*, 936–948.

Kouzarides, T. (2000). Acetylation: a regulatory modification to rival phosphor-ylation? EMBO J. *19*, 1176–1179.

Kouzarides, T. (2007). Chromatin modifications and their function. Cell *128*, 693–705.

Lane, A.A., and Chabner, B.A. (2009). Histone deacetylase inhibitors in cancer therapy. J. Clin. Oncol. *27*, 5459–5468.

Laskowski, R.A., MacArthur, M.W., Moss, D.S., and Thornton, J.M. (1993). PROCHECK: a program to check the stereochemical quality of protein struc-tures. J. Appl. Crystallogr. *26*, 283–291.

Li, Y., Wen, H., Xi, Y., Tanaka, K., Wang, H., Peng, D., Ren, Y., Jin, Q., Dent, S.Y.R., Li, W., et al. (2014). AF9 YEATS domain links histone acetylation to DOT1L-mediated H3K79 methylation. Cell *159*, 558–571.

Liu, B., Lin, Y., Darwanto, A., Song, X., Xu, G., and Zhang, K. (2009). Identification and characterization of propionylation at histone H3 lysine 23 in mammalian cells. J. Biol. Chem. *284*, 32288–32295.

Lu, C., and Thompson, C.B. (2012). Metabolic regulation of epigenetics. Cell Metab. *16*, 9–17.

Lubula, M.Y., Eckenroth, B.E., Carlson, S., Poplawski, A., Chruszcz, M., and Glass, K.C. (2014). Structural insights into recognition of acetylated histone ligands by the BRPF1 bromodomain. FEBS Lett. *588*, 3844–3854.

Lucas, X., Wohlwend, D., Hugle, M., Schmidtkunz, K., Gerhardt, S., Schule, R., Jung, M., Einsle, O., and Gunther, S. (2013). 4-Acyl pyrroles: mimicking acet-ylated lysines in histone code reading. Angew. Chem. Int. Ed. Engl. *52*, 14055–14059.

Masri, S., Zocchi, L., Katada, S., Mora, E., and Sassone-Corsi, P. (2012). The circadian clock transcriptional complex: metabolic feedback intersects with epigenetic control. Ann. N. Y. Acad. Sci. *1264*, 103–109.

Masri, S., Patel, V.R., Eckel-Mahan, K.L., Peleg, S., Forne, I., Ladurner, A.G., Baldi, P., Imhof, A., and Sassone-Corsi, P. (2013). Circadian acetylome reveals regulation of mitochondrial metabolic pathways. Proc. Natl. Acad. Sci. USA *110*, 3339–3344.

McBrian, M.A., Behbahan, I.S., Ferrari, R., Su, T., Huang, T.W., Li, K., Hong, C.S., Christofk, H.R., Vogelauer, M., Seligson, D.B., et al. (2013). Histone acet-ylation regulates intracellular pH. Mol. Cell *49*, 310–321.

McCoy, A.J., Grosse-Kunstleve, R.W., Adams, P.D., Winn, M.D., Storoni, L.C., and Read, R.J. (2007). Phaser crystallographic software. J. Appl. Crystallogr. *40*, 658–674.

Minor, W., Cymborowski, M., Otwinowski, Z., and Chruszcz, M. (2006). HKL-3000: the integration of data reduction and structure solution—from diffraction images to an initial model in minutes. Acta Crystallogr. D Biol. Crystallogr. *62*, 859–866.

Morinière, J., Rousseaux, S., Steuerwald, U., Soler-Lopez, M., Curtet, S., Vitte, A.L., Govin, J., Gaucher, J., Sadoul, K., Hart, D.J., et al. (2009). Cooperative binding of two acetylation marks on a histone tail by a single bromodomain. Nature *461*, 664–668.

Newman, J.C., He, W., and Verdin, E. (2012). Mitochondrial protein acylation and intermediary metabolism: regulation by sirtuins and implications for meta-bolic disease. J. Biol. Chem. *287*, 42436–42443.

Norris, K.L., Lee, J.Y., and Yao, T.P. (2009). Acetylation goes global: the emer-gence of acetylation biology. Sci. Signal. *2*, pe76.

Olsen, C.A. (2014). An update on lysine deacylases targeting the expanding "acylome". ChemMedChem *9*, 434–437.

Owen, D.J., Ornaghi, P., Yang, J.C., Lowe, N., Evans, P.R., Ballario, P., Neuhaus, D., Fileticii, P., and Travers, A.A. (2000). The structural basis for the recognition of acetylated histone H4 by the bromodomain of histone acetyl-transferase gcn5p. EMBO J. *19*, 6141–6149.

Park, J., Chen, Y., Tishkoff, D.X., Peng, C., Tan, M., Dai, L., Xie, Z., Zhang, Y., Zwaans, B.M., Skinner, M.E., et al. (2013). SIRT5-mediated lysine desucciny-lation impacts diverse metabolic pathways. Mol. Cell *50*, 919–930.

Peng, C., Lu, Z., Xie, Z., Cheng, Z., Chen, Y., Tan, M., Luo, H., Zhang, Y., He, W., Yang, K., et al. (2011). The first identification of lysine malonylation sub-strates and its regulatory enzyme. Mol. Cell Proteomics *10*, M111.012658.

Potterton, E., McNicholas, S., Krissinel, E., Cowtan, K., and Noble, M. (2002). The CCP4 molecular-graphics project. Acta Crystallogr. D Biol. Crystallogr. *58*, 1955–1957.

Sabari, B.R., Tang, Z., Huang, H., Yong-Gonzalez, V., Molina, H., Kong, H.E., Dai, L., Shimada, M., Cross, J.R., Zhao, Y., et al. (2015). Intracellular crotonyl-CoA stimulates transcription through p300-catalyzed histone crotonylation. Mol. Cell *58*, 203–215.

Sanchez, R., Meslamani, J., and Zhou, M.M. (2014). The bromodomain: from epigenome reader to druggable target. Biochim. Biophys. Acta *1839*, 676–685.

Shahbazian, M.D., and Grunstein, M. (2007). Functions of site-specific histone acetylation and deacetylation. Annu. Rev. Biochem. *76*, 75–100.

Shi, J., and Vakoc, C.R. (2014). The mechanisms behind the therapeutic activ-ity of BET bromodomain inhibition. Mol. Cell *54*, 728–736.

Smith, B.C., and Denu, J.M. (2007). Acetyl-lysine analog peptides as mecha-nistic probes of protein deacetylases. J. Biol. Chem. *282*, 37256–37265.

Smith, K.T., and Workman, J.L. (2009). Introducing the acetylome. Nat. Biotechnol. *27*, 917–919.

Tan, M., Luo, H., Lee, S., Jin, F., Yang, J.S., Montellier, E., Buchou, T., Cheng, Z., Rousseaux, S., Rajagopal, N., et al. (2011). Identification of 67 histone marks and histone lysine crotonylation as a new type of histone modification. Cell 146, 1016–1028.

Tan, M., Peng, C., Anderson, K.A., Chhoy, P., Xie, Z., Dai, L., Park, J., Chen, Y., Huang, H., Zhang, Y., et al. (2014). Lysine glutarylation is a protein posttranslational modification regulated by SIRT5. Cell Metab. 19, 605–617.

Tweedie-Cullen, R.Y., Brunner, A.M., Grossmann, J., Mohanna, S., Sichau, D., Nanni, P., Panse, C., and Mansuy, I.M. (2012). Identification of combinatorial patterns of post-translational modifications on individual histones in the mouse brain. PLoS One 7, e36980.

Vidler, L.R., Brown, N., Knapp, S., and Hoelder, S. (2012). Druggability analysis and structural classification of bromodomain acetyl-lysine binding sites. J. Med. Chem. 55, 7346–7359.

Vollmuth, F., and Geyer, M. (2010). Interaction of propionylated and butyrylated histone H3 lysine marks with Brd4 bromodomains. Angew. Chem. Int. Ed. Engl. 49, 6768–6772.

Vollmuth, F., Blankenfeldt, W., and Geyer, M. (2009). Structures of the dual bromodomains of the P-TEFb-activating protein Brd4 at atomic resolution. J. Biol. Chem. 284, 36547–36556.

Wagner, G.R., and Payne, R.M. (2013). Widespread and enzyme-independent Nepsilon-acetylation and Nepsilon-succinylation of proteins in the chemical conditions of the mitochondrial matrix. J. Biol. Chem. 288, 29036–29045.

Weinert, B.T., Wagner, S.A., Horn, H., Henriksen, P., Liu, W.R., Olsen, J.V., Jensen, L.J., and Choudhary, C. (2011). Proteome-wide mapping of the Drosophila acetylome demonstrates a high degree of conservation of lysine acetylation. Sci. Signal. 4, ra48.

Weinert, B.T., Scholz, C., Wagner, S.A., Iesmantavicius, V., Su, D., Daniel, J.A., and Choudhary, C. (2013). Lysine succinylation is a frequently occurring modification in prokaryotes and eukaryotes and extensively overlaps with acetylation. Cell Rep. 4, 842–851.

Wen, H., Li, Y., Xi, Y., Jiang, S., Stratton, S., Peng, D., Tanaka, K., Ren, Y., Xia, Z., Wu, J., et al. (2014). ZMYND11 links histone H3.3K36me3 to transcription elongation and tumour suppression. Nature 508, 263–268.

Winn, M.D., Murshudov, G.N., and Papiz, M.Z. (2003). Macromolecular TLS refinement in REFMAC at moderate resolutions. Methods Enzymol. 374, 300–321.

Wisniewski, J.R., Zougman, A., and Mann, M. (2008). Nepsilon-formylation of lysine is a widespread post-translational modification of nuclear proteins occurring at residues involved in regulation of chromatin function. Nucleic Acids Res. 36, 570–577.

Xie, Z., Dai, J., Dai, L., Tan, M., Cheng, Z., Wu, Y., Boeke, J.D., and Zhao, Y. (2012). Lysine succinylation and lysine malonylation in histones. Mol. Cell Proteomics 11, 100–107.

Xing, S., and Poirier, Y. (2012). The protein acetylome and the regulation of metabolism. Trends Plant Sci. 17, 423–430.

Zeng, L., Zhang, Q., Li, S., Plotnikov, A.N., Walsh, M.J., and Zhou, M.M. (2010). Mechanism and regulation of acetylated histone binding by the tandem PHD finger of DPF3b. Nature 466, 258–262.

Zhang, K., Chen, Y., Zhang, Z., and Zhao, Y. (2009). Identification and verification of lysine propionylation and butyrylation in yeast core histones using PTMap software. J. Proteome Res. 8, 900–906.

Zhao, S., Xu, W., Jiang, W., Yu, W., Lin, Y., Zhang, T., Yao, J., Zhou, L., Zeng, Y., Li, H., et al. (2010). Regulation of cellular metabolism by protein lysine acetylation. Science 327, 1000–1004.